Title

In Vivo Fluorescence Imaging of Gastrointestinal Stromal Tumors Using Fluorophore-Conjugated Anti-KIT Antibody

Journal

Annals of Surgical Oncology, 20(Suppl 3)

ISSN

1068-9265

Authors

Metildi, Cristina A
Tang, Chih-Min
Kaushal, Sharmeela
et al.

Publication Date

2013-12-01

DOI

10.1245/s10434-013-3172-6

Peer reviewed

Published in final edited form as:
Ann Surg Oncol. 2013 December ; 20(0 3): S693–S700. doi:10.1245/s10434-013-3172-6.

In Vivo Fluorescence Imaging of Gastrointestinal Stromal Tumors Using Fluorophore-Conjugated Anti-KIT Antibody

Cristina A. Metildi, MD[1], **Chih-Min Tang, PhD**[1], **Sharmeela Kaushal, PhD**[1], **Stephanie Y. Leonard, BA**[1], **Paolo Magistri, MD**[1], **Hop S. Tran Cao, MD**[1], **Robert M. Hoffman, PhD**[1,2], **Michael Bouvet, MD**[1], and **Jason K. Sicklick, MD**[1]

Jason K. Sicklick: jsicklick@ucsd.edu

[1]Division of Surgical Oncology, Department of Surgery, University of California, San Diego, CA

[2]AntiCancer, Inc., San Diego, CA

Abstract

Background—Gastrointestinal stromal tumors (GISTs) are frequently characterized by KIT overexpression. Tumor-free margins and complete cytoreduction of disease are mainstays of treatment. We hypothesized that fluorescently labeled anti-KIT antibodies can label GIST in vivo.

Methods—KIT K641E$^{+/-}$ transgenic mice that spontaneously develop cecal GISTs were used in this study, with C57BL/6 mice serving as controls. Alexa 488 fluorophore-conjugated anti-KIT antibodies were delivered via the tail vein 24 h prior to fluorescence imaging. Following fluorescence laparoscopy, mice were sacrificed. The gastrointestinal tracts were grossly examined for tumors followed by fluorescence imaging. Tumors were harvested for histologic confirmation.

Results—KIT K641E$^{+/-}$ mice and C57BL/6 control mice received anti-KIT antibody or isotope control antibody. Fluorescence laparoscopy had a high tumor signal-to-background noise ratio. Upon blinded review of intravital fluorescence and bright light images, there were 2 false-positive and 0 false-negative results. The accuracy was 92 %. The sensitivity, specificity, positive and negative predictive values were 100, 87, 85, and 100 %, respectively, for the combined modalities.

Conclusions—In this study, we present a method for in vivo fluorescence labeling of GIST in a murine model. Several translatable applications include: laparoscopic staging; visualization of peritoneal metastases; assessment of margin status; endoscopic differentiation of GISTs from other benign submucosal tumors; and longitudinal surveillance of disease response. This novel approach has clear clinical applications that warrant further research and development.

Gastrointestinal stromal tumor (GIST), the most common mesenchymal tumor of the gut, is often characterized by high expression of KIT.[1,2] While these submucosal neoplasms can

Cristina A. Metildi and Chih-Min Tang have contributed equally to this article.

Presented at the 2013 Society of Surgical Oncology Annual Cancer Symposium, March 6–9, 2013, National Harbor, MD.

Electronic supplementary material The online version of this article (doi:10.1245/s10434-013-3172-6) contains supplementary material, which is available to authorized users.

DISCLOSURE Dr. Sicklick is a consultant to Novartis Pharmaceuticals. Dr. Hoffman is a non-salaried president and a stockholder in AntiCancer Inc. The remaining authors have no relevant financial disclosures.

arise anywhere in the gastrointestinal tract, they most frequently occur in the stomach (40–70 %) and small bowel (20–40 %).[3,4] GISTs arise from the gut pacemaker cells, also known as the interstitial cells of Cajal (ICC). Both GISTs and ICCs express KIT (c-KIT, CD117) while KIT mutations frequently drive GIST sarcomagenesis.[4] However, other submucosal tumors (SMTs), such as schwannomas, leiomyomas, and pancreatic rests can be mistaken for GISTs based upon location and imaging characteristics. In the absence of a tissue diagnosis, some patients may undergo unnecessary surgical resections. However, for patients with GIST, R0 resection (i.e., tumor-free margins) is the mainstay of treatment. But even in cases where this is achieved, the risk of metastatic disease is substantial.[5,6] This frequently involves the liver and/or peritoneal surfaces due to hema-togenous spread and peritoneal seeding, respectively.[7,8]

While patients with imatinib-sensitive metastatic GIST have better outcomes than those patients that have disease progression on imatinib therapy (Gleevec, Novartis, Basel, Switzerland), the additional benefit of surgery over imatinib alone is still unproven.[9,10] But even in the pre-imatinib era, completeness of cytoreduction for metastatic GIST had a significant impact on prognosis.[11] Therefore, methods to improve visualization of peritoneal based metastases may be advantageous for the surgical treatment of GIST.

We hypothesized that several of the aforementioned issues involving the diagnosis and treatment of GIST may be addressed by developing a real-time method for in vivo fluorescence imaging of GIST. There are several translatable applications including endoscopic differentiation of GISTs from other benign SMTs, laparoscopic staging along with identification of peritoneal metastases, and assessment of margin status. Herein, we describe the first method for in vivo fluorescence labeling and visualization of GIST using fluorophore-conjugated anti-KIT antibodies, which can be intravenously administered to transgenic mice with GISTs.

MATERIALS AND METHODS

Antibody Conjugation

Monoclonal antibody specific for KIT (Wistar rat anti-mouse monoclonal antibody; isotype: IgG_{2b}, j, #553352) and IgG isotype control antibody were obtained from BD Pharmingen (San Jose, CA). The antibody was labeled with the AlexaFluor 488 Protein Labeling Kit (Molecular Probes, Grand Island, NY) according to the manufacturer's instructions and as previously described.[12] Briefly, the monoclonal antibody was reconstituted at 1 mg/mL in 0.1 M sodium bicarbonate. One hundred μL of the solution was added to the reactive dye. This was allowed to incubate for 1 h at room temperature. The conjugated antibody was then separated from the remaining unconjugated dye on a gravity purification column. Antibody and dye concentrations in the final sample were determined using spectrophotometric absorbance analyses.

Animal Care

Male and female KIT $K641E^{+/-}$ mice (kindly provided by B. Rubin, Cleveland Clinic, OH) and C57BL/6 mice were maintained in a barrier facility on high-efficiency particulate air-

filtered racks and fed autoclaved laboratory rodent diet (Teckland LM-485; Western Research Products, Laramie, WY). Mice were started on an alfalfa-free diet (Teckland 2016) 7 days prior to imaging and were nil per os (NPO) for 24 h prior to the procedure. Surgical procedures were performed under anesthesia using 100 μL of a ketamine and xylazine mixture and 20 μL of 1 mg/kg buprenorphine for pain control. Euthanasia was achieved by 100 % carbon dioxide inhalation, followed by cervical dislocation. All animal studies were approved by the UCSD Institutional Animal Care and Use Committee and conducted in accordance with the principles and procedures outlined in the National Institutes of Health (NIH) Guide for the Care and Use of Animals.

Fluorescence Laparoscopy

A standard laparoscopic tower, provided by Stryker (Kalamazoo, MI), was modified in the following manner to achieve fluorescence laparoscopy. The excitation light source, a Stryker L9000 light-emitting diode (LED) lamp, was filtered through a glass emission filter (Schott GG495) placed between the laparoscope and the Stryker 1288 HD camera. Using the computer software system provided by Stryker, adjustments to the red, blue, and green components of the Stryker L9000 LED light source were made to allow for visualization of the fluorescent tumors. A Stryker X8000 xenon light source was used for bright light laparoscopy as reported.[13] Fluorescence laparoscopic images were obtained. We used ImageJ software v1.440 (NIH, Bethesda, MD) to calculate fluorescence signal intensities of the background and the Alexa 488-labeled GISTs.

Tumor Labeling

Twenty-four hours prior to imaging, mice received 50–100 μg of Alexa 488-conjugated anti-KIT antibody via tail vein injection. The dose and timing of injection were derived from a previous in vivo study.[14] A total of 13 mice were used in this study. Seven of the mice had a KIT mutation (KIT $K641E^{+/-}$) based on genotyping and 6 were wild-type (C57BL/6) mice.[15] Twenty-four hours prior to laparoscopy, 4 KIT $K641E^{+/-}$ mice and 3 C57BL/6 mice received an injection of 50–100 μg of anti-KIT-Alexa 488 via the tail vein. The remaining mice received IgG isotype-Alexa 488.

Mouse Laparoscopy

Laparoscopy on mice was performed as previously described.[13] A standard staging laparoscopy procedure was performed. All four quadrants of the peritoneal cavity were examined in a systematic fashion. Each mouse was examined under two light modes: fluorescence laparoscopy using the Stryker L9000 LED light source and bright light using the Stryker X8000 xenon light source. A pediatric laparoscopic grasper was inserted in the left lower quadrant for bowel mobilization in order to visualize the cecum. At the termination of laparoscopy, mice were sacrificed and their abdominal cavities exposed for OV-100 (Olympus, Center Valley, PA) imaging.

Histopathology

At necropsy, all identified lesions were collected. Small tumor foci observed during in vivo fluorescence laparoscopic imaging were localized post-mortem in fresh ex vivo organ blocks

using both bright light and fluorescence imaging. Serial sections of formalin-fixed, paraffin-embedded tissue were used for hematoxylin and eosin (H&E) staining, as well as immunohistochemistry. For all tumors, the histological diagnoses were confirmed under light microscopy.

Immunohistochemistry

Serial sections of formalin-fixed, paraffin-embedded tumors, 10 μm thick, were used for immunohistochemical staining. The sections were treated twice with 0.3 % Triton X-100 (Sigma-Aldrich, St. Louis, MO) in phosphate-buffered saline for 10 min and then in 0.3 % hydrogen peroxide solution in order to block endogenous peroxidase activity. The sections were then blocked with serum followed by an avidin-biotin blocking reagent (Vector Laboratories; Burlingame, CA) to inhibit nonspecific binding in the tissue. The sections were then incubated with polyclonal rabbit anti-human CD117 (c-KIT) antibody (1:50, #A450229-2, Dako; Carpinteria, CA) overnight at 4 °C. This antibody cross-reacts with mouse KIT. Sections were next incubated with biotinylated secondary antibody and ABC reagents of the Vectastain Elite Universal ABC kit according to the manufacturer's instructions (Vector Laboratories). The secondary antibody was detected using the avidin-biotin-peroxidase method with 3,3′-diam-inobenzidine as the substrate (Vector Laboratories). Negative controls were performed by omitting the primary antibody and/or using isotype control antibody. These controls revealed minimal or no background staining (data not shown).

Data Processing and Statistical Analysis

All images obtained were not processed in any manner. Representative frames are presented. Intravital images were obtained with the OV-100 imaging system and served to confirm laparoscopic findings. PASW Statistics 18.0 (SPSS, Armonk, NY) was used for statistical analysis of fluorescence signal intensities of background and fluorescent antibody-labeled tumor. Data are expressed as mean ± standard error of mean. A Welch's *t*-test was used to compare the continuous variables between the two groups. P-value <0.05 was considered statistically significant for all comparisons. Analyses to determine accuracy, sensitivity, specificity, positive predictive value (PPV), and negative predictive value (NPV) were performed using the bright light and fluorescence methods. Reported results were calculated by combining both imaging methods to determine tumor presence, visualization and fluorescent antibody-labeling.

RESULTS

Primary Tumor Detection

The KIT K641E$^{+/-}$ transgenic mice spontaneously develop cecal GISTs (Fig. 1). At approximately 4–8 months of age, four mice were injected via the tail vein with 50–100 μg of anti-KIT-Alexa 488. Another three transgenic mice were injected with IgG isotype control antibody to serve as a negative control. Pneumoperitoneum was established to allow adequate distension of the abdominal wall for visualization and navigation. All quadrants were evaluated in a systematic manner. To assist with cecal visualization of tumors and

bowel mobilization, a pediatric laparoscopic grasper was inserted into the left lower quadrant.[15]

Fluorescence laparoscopy, achieved by filtering the LED light source through a 495-nm filter, enabled real-time visualization and detection of the fluorescently labeled cecal GISTs (Fig. 2a–b, Supplemental Video). In addition, with adjustments to the LED light components, adequate contrast was achieved to permit distinction of the fluorescently labeled tumor tissue from the autofluorescence of normal surrounding bowel. This made tumor detection more efficacious. The accurate binding capability of the fluorophore-conjugated anti-KIT antibody provided adequate fluorescent brightness, which afforded the appropriate tumor signal-to-background noise ratio (Fig. 2c) for accurate tumor detection and localization. The mean fluorescence signal was determined using ImageJ. The fluorescence signal intensity was calculated from images obtained during fluorescence laparoscopy. Laparoscopic images (N = 7–16) were obtained from GIST-bearing mice injected with the anti-KIT-488 antibody. Randomly selected areas of the fluorescently labeled tumor and the surrounding bowel were measured from these images in order to yield 15 values for the tumor and the background bowel. The mean fluorescence signal intensity of the fluorescent antibody-labeled tumor (55.2 ± 4.7) was significantly greater than that of the surrounding background (23.2 ± 2.3, $P < 0.001$). Fluorescence laparoscopy combined with fluorophore-conjugated anti-KIT antibody afforded a 2.4-fold increase in the fluorescence signal intensity over background. This allowed for detection of GISTs in all tumor-bearing mice (4 of 4), yielding an accuracy of 100 %.

Postlaparoscopy Analysis

Upon completion of laparoscopy, the mice were sacrificed and their abdominal cavities were exposed for imaging with the OV-100 Imaging System using a green fluorescent protein filter. The OV-100 images served as a positive control against which to compare the laparoscopic findings. After imaging, all lesions identified under both light modes were collected when possible and verified histologically. Furthermore, three C57BL/6 (tumor-free) mice were injected with anti-KIT-Alexa 488 and another three C57BL/6 mice with IgG to serve as a negative control.

On intravital OV-100 imaging, Alexa 488 labeling with the KIT antibody accurately detected GISTs in all four of the mice with GIST tumors (Fig. 3a, *i–iv* and b, *iii*). H&E and KIT (Fig. 3a, *v–vi*) staining confirmed the presence of tumor in all four mice. This labeling was not achieved when the IgG isotype antibody was used (Fig. 3b, *ii*,*iv*). In addition, there was no fluorescence labeling with anti-KIT antibody in the three non-tumor-bearing mice (Fig. 3b, *i*). Bright light and fluorescence imaging results are summarized in Tables 1 and 2, respectively. There were no false negatives but two false positives-one transgenic mouse injected with IgG and one wild-type mouse injected with IgG-yielding an accuracy of 92 %. Combining bright light visualization with a fluorescent dye conjugated to anti-KIT antibody yielded a PPV of 85 %, NPV of 100 %, specificity of 87 %, and sensitivity of 100 %.

DISCUSSION

In recent years, there has been growing interest in in situ tumor imaging techniques that utilize fluorescent antibodies, fluorescent peptides, as well as viruses that deliver genetic reporters.[12–14,16,17] The improved detection of tumors as well as the enhanced visualization of tumor margins offered by these approaches have many potential applications in the diagnosis and treatment of cancers. In the present study, we demonstrated a novel method for using a fluorescent antibody against a commonly overex-pressed GIST antigen, KIT (c-KIT, CD117), in order to label these tumors in a transgenic mouse model.

The optimal method for treating GIST is complete surgical resection with negative microscopic margins (e.g., R0 resection) and an intact pseudocapsule without tumor rupture. This correlates with improved progression-free survival and overall survival.[5,6] Targeting tumors via methods that fluorescently label cancer cells has been demonstrated to improve R0 resection rates in mouse models of cancer.[18,19] By enhancing the surgeon's ability to accurately and more objectively delineate tumor margins, more effective removal of cancer cells can be achieved. In turn, this leads to lower recurrence rates, longer disease-free survival and improved overall survival in several mouse models that have been studied.[18–20] For patients with GIST, McCarter et al.[21] recently demonstrated that those undergoing R0 and R1 resections had no difference in rates of local recurrences, irrespective of receiving adjuvant imatinib therapy for 1 year. Thus, while our technique may not further decrease the already low local recurrence rates, it may help detect occult distant metastatic disease at the time of initial resection.

Fluorophore-conjugated antibodies against KIT can accurately label KIT-expressing GISTs for detection of primary tumors, as well as small metastatic deposits that may be missed at the time of surgical resection. Enhancing detection and visualization of peritoneal metastasis can also significantly improve cytoreductive efforts in these patients. Fifteen to 47 % of patients diagnosed with GIST present with overt metastatic disease to the liver and peritoneum.[22] Although the tyrosine kinase inhibitor i-matinib has been quite effective in treating locally advanced, unresectable, and metastatic GIST, there is a clear role for surgical resection following imatinib treatment.[9,23–26] A recent retrospective review comparing outcomes in patients treated with surgical resection after imatinib versus patients treated with imatinib alone demonstrated longer progression-free survival and overall survival in the surgery plus imatinib group.[10] Thus, enhancing surgical resection in primary and metastatic disease using fluorescence labeling of the tumors may improve outcomes.

This study is a proof of concept in order to confirm the hypothesis that GISTs can be fluorescently labeled in vivo as well as viewed laparoscopically, although we report two false-positive reads with fluorescence imaging and none with bright light review. While a visible bowel tumor is obvious, developing the first method for identifying sub-clinical disease is the ultimate goal. We employed the current model because it is highly reproducible and consistent. This avoided the potential for missing occult disease during this initial phase of methodology development. Future experiments with orthotopic transplant models of human GIST cell line using immunodeficient mice injected with GIST cell lines are in order to recapitulate peritoneal-based disease.

GISTs are often diagnosed incidentally on CT or upper endoscopy. While CT is the imaging modality of choice for the detection, staging, surgical planning and follow-up of patients with GIST, it may not accurately identify peritoneal seeding, a common form of metastasis in these patients.[27] Thus, the use of fluorophore-conjugated antibodies against KIT can provide non-radioactive imaging potential to aid in the diagnosis and treatment planning of GIST. Moreover, it may also be utilized for following disease response by simply detecting a decrease in fluorescence. Such a concept was recently reported by Edris and colleagues[28] wherein they used a monoclonal antibody against KIT, similar to what was utilized in this study, to treat imatinib-resistant GISTs. They genetically engineered human GIST cell lines that expressed green fluorescent protein (GFP) in vitro. With fluorescence microscopy, this group was able to evaluate the presence of GFP-positive xenograft growth and utilize fluorescence as a biomarker of treatment response. In the current study, we demonstrate the application of fluorescence laparoscopy with anti-KIT-Alexa 488 antibodies to accurately identify GISTs in vivo using a transgenic mouse model. Thus, a clinical application of our method may include longitudinally following treatment responses in GIST patients.

Endoscopy with fine needle aspiration or core needle biopsy is another important method of diagnosing GIST because these tumors can be confused with a variety of other SMTs such as leiomyomas and schwannomas. One major distinguishing factor is that the latter tumors are almost uniformly reported as KIT-negative. However, it is also noteworthy that about one in 20 GISTs also do not stain for KIT despite otherwise resembling KIT-positive GISTs.[29,30] Fluorophore-conjugated antibodies to KIT may enhance endoscopic differentiation of GISTs from these SMTs without the need for biopsy.

Although our study has limitations including the challenges encountered from bowel autofluorescence, and the consistent location of cecal tumor development in this transgenic mouse model, there remain several translatable applications. This novel method for in vivo fluorescence imaging of GIST may be used for identification of peritoneal metastases and following the disease response. It can also provide a non-radioactive imaging option for diagnostic purposes such as endoscopic differentiation of GISTs from benign SMTs. Finally, fluorescently labeling GISTs with conjugated antibodies to KIT may aid in laparoscopic staging, as well as assessment of margin status for improved resection rates and surgical outcomes. Taken together, this novel approach has clear clinical applications that warrant further research and development.

Supplementary Material

Refer to Web version on PubMed Central for supplementary material.

Acknowledgments

The authors thank Dr. Jurg Rohrer (BD Pharmingen) for providing anti-KIT and isotype control antibodies. This work was supported in part by the National Cancer Institute CA142669 and CA132971 (to Dr. Bouvet and AntiCancer Inc.), as well as T32CA121938 (to Dr. Metildi).

REFERENCES

1. Miettinen M, Majidi M, Lasota J. Pathology and diagnostic criteria of gastrointestinal stromal tumors (GISTs): a review. Eur J Cancer. 2002; 38(Suppl 5):S39–S51. [PubMed: 12528772]
2. Demetri GD, von Mehren M, Antonescu CR, et al. NCCN Task Force report: update on the management of patients with gastrointestinal stromal tumors. J Natl Compr Canc Netw. 2010; 8(Suppl 2):S1–S41. [PubMed: 20457867]
3. Nilsson B, Bumming P, Meis-Kindblom JM, et al. Gastrointestinal stromal tumors: the incidence, prevalence, clinical course, and prognostication in the preimatinib mesylate era—a population-based study in western Sweden. Cancer. 2005; 103:821–829. [PubMed: 15648083]
4. Corless CL, Barnett CM, Heinrich MC. Gastrointestinal stromal tumours: origin and molecular oncology. Nat Rev Cancer. 2011; 11:865–878. [PubMed: 22089421]
5. Dematteo RP, Ballman KV, Antonescu CR, et al. Adjuvant i-matinib mesylate after resection of localised, primary gastrointestinal stromal tumour: a randomised, double-blind, placebo-controlled trial. Lancet. 2009; 373(9669):1097–1104. [PubMed: 19303137]
6. Joensuu H, Eriksson M, Sundby Hall K, et al. One vs three years of adjuvant imatinib for operable gastrointestinal stromal tumor: a randomized trial. JAMA. 2012; 307:1265–1272. [PubMed: 22453568]
7. Chourmouzi D, Sinakos E, Papalavrentios L, Akriviadis E, Drevelegas A. Gastrointestinal stromal tumors: a pictorial review. Gastrointestin Liver Dis. 2009; 18:379–383.
8. Miettinen M, Lasota J. Gastrointestinal stromal tumors: review on morphology, molecular pathology, prognosis, and differential diagnosis. Arch Pathol Lab Med. 2006; 130:1466–1478. [PubMed: 17090188]
9. Eisenberg BL, Harris J, Blanke CD, et al. Phase II trial of neo-adjuvant/adjuvant imatinib mesylate (IM) for advanced primary and metastatic/recurrent operable gastrointestinal stromal tumor (GIST): early results of RTOG 0132/ACRIN 6665. J Surg Oncol. 2009; 99:42–7. [PubMed: 18942073]
10. Park S, Ryu MH, Ryoo BY, et al. The role of surgical resection following imatinib treatment in patients with metastatic or recurrent GIST. J Clin Oncol. 2012; 30(Suppl) abstract 62.
11. Yan H, Marchettini P, Acherman YI, Gething SA, Brun E, Sugarbaker PH. Prognostic assessment of gastrointestinal stromal tumor. Am J Clin Oncol. 2003; 26:221–228. [PubMed: 12796588]
12. Kaushal S, McElroy MK, Luiken GA, et al. Fluorophore-conjugated anti-CEA antibody for the intraoperative imaging of pancreatic and colorectal cancer. J Gastrointest Surg. 2008; 12:1938–1950. [PubMed: 18665430]
13. Metildi CA, Kaushal S, Lee C, et al. An LED light source and novel fluorophore combinations improve fluorescence laparoscopic detection of metastatic pancreatic cancer in orthotopic mouse models. J Am Coll Surg. 2012; 214:997–1007. e1002. [PubMed: 22542065]
14. McElroy M, Kaushal S, Luiken GA, et al. Imaging of primary and metastatic pancreatic cancer using a fluorophore-conjugated anti-CA19-9 antibody for surgical navigation. World J Surg. 2008; 32:1057–1066. [PubMed: 18264829]
15. Rubin BP, Antonescu CR, Scott-Browne JP, et al. A knock-in mouse model of gastrointestinal stromal tumor harboring kit K641E. Cancer Res. 2005; 65:6631–6639. [PubMed: 16061643]
16. Kishimoto H, Zhao M, Hayashi K, et al. In vivo internal tumor illumination by telomerase-dependent adenoviral GFP for precise surgical navigation. Proc Natl Acad Sci USA. 2009; 106:14514–14517. [PubMed: 19706537]
17. Olson ES, Jiang T, Aguilera TA, et al. Activatable cell penetrating peptides linked to nanoparticles as dual probes for in vivo fluorescence and MR imaging of proteases. Proc Natl Acad Sci USA. 2010; 107:4311–4316. [PubMed: 20160077]
18. Metildi CA, Kaushal S, Hardamon CR, et al. Fluorescence-guided surgery allows for more complete resection of pancreatic cancer, resulting in longer disease-free survival compared with standard surgery in orthotopic mouse models. J Am Coll Surg. 2012; 215:126–135. [PubMed: 22632917]
19. Metildi CA, Kaushal S, Snyder CS, Hoffman RM, Bouvet M. Fluorescence-guided surgery of human colon cancer increases complete resection resulting in cures in an orthotopic nude mouse model. J Surg Res. 2013; 179:87–93. [PubMed: 23079571]

20. Jiang T, Olson ES, Nguyen QT, Roy M, Jennings PA, Tsien RY. Tumor imaging by means of proteolytic activation of cell-penetrating peptides. Proc Natl Acad Sci USA. 2004; 101:17867–17872. [PubMed: 15601762]
21. McCarter MD, Antonescu CR, Ballman KV, et al. Microscopically positive margins for primary gastrointestinal stromal tumors: analysis of risk factors and tumor recurrence. J Am Coll Surg. 2012; 215:53–59. [PubMed: 22726733]
22. DeMatteo RP, Lewis JJ, Leung D, Mudan SS, Woodruff JM, Brennan MF. Two hundred gastrointestinal stromal tumors: recurrence patterns and prognostic factors for survival. Ann Surg. 2000; 231:51–58. [PubMed: 10636102]
23. Rubin BP, Heinrich MC, Corless CL. Gastrointestinal stromal tumour. Lancet. 2007; 369(9574): 1731–1741. [PubMed: 17512858]
24. Learn PA, Sicklick JK, DeMatteo RP. Randomized clinical trials in gastrointestinal stromal tumors. Surg Oncol Clin North Am. 2010; 19:101–113.
25. Raut CP, Posner M, Desai J, et al. Surgical management of advanced gastrointestinal stromal tumors after treatment with targeted systemic therapy using kinase inhibitors. J Clin Oncol. 2006; 24:2325–2331. [PubMed: 16710031]
26. Raut CP, Wang Q, Manola J, et al. Cytoreductive surgery in patients with metastatic gastrointestinal stromal tumor treated with sunitinib malate. Ann Surg Oncol. 2010; 17:407–415. [PubMed: 19898902]
27. Reichardt P, Blay JY, Mehren M. Towards global consensus in the treatment of gastrointestinal stromal tumor. Exp Rev Anti-cancer Ther. 2010; 10:221–232.
28. Edris B, Willingham SB, Weiskopf K, et al. Anti-KIT monoclonal antibody inhibits imatinib-resistant gastrointestinal stromal tumor growth. Proc Natl Acad Sci USA. 2013; 110:3501–3506. [PubMed: 23382202]
29. Medeiros F, Corless CL, Duensing A, et al. KIT-negative gastrointestinal stromal tumors: proof of concept and therapeutic implications. Am J Surg Pathol. 2004; 28:889–894. [PubMed: 15223958]
30. Orosz Z, Tornoczky T, Sapi Z. Gastrointestinal stromal tumors: a clinicopathologic and immunohistochemical study of 136 cases. Pathol Oncol Res. 2005; 11:11–21. [PubMed: 15800677]

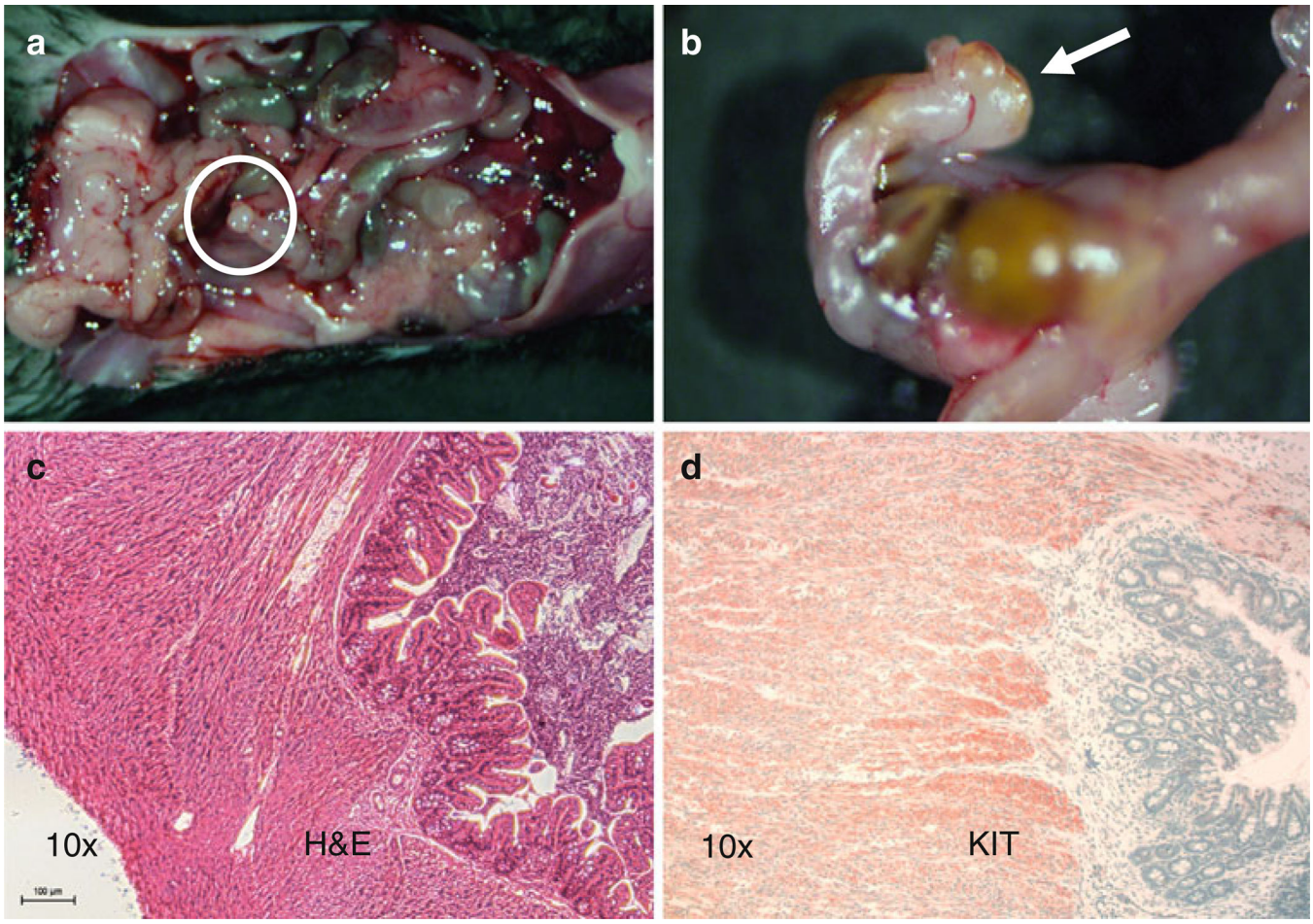

FIG. 1.

Transgenic mouse model of GIST. **a** Image of a KIT K641E$^{+/-}$ mouse at necropsy demonstrating the presence of a cecal GIST. Upon magnification (**b**), the cecal tumor is visualized (arrow). **c** Hematoxylin and eosin staining confirms the presence of a spindle cell neoplasm. Positive KIT immunostaining (**d**) is consistent with a GIST

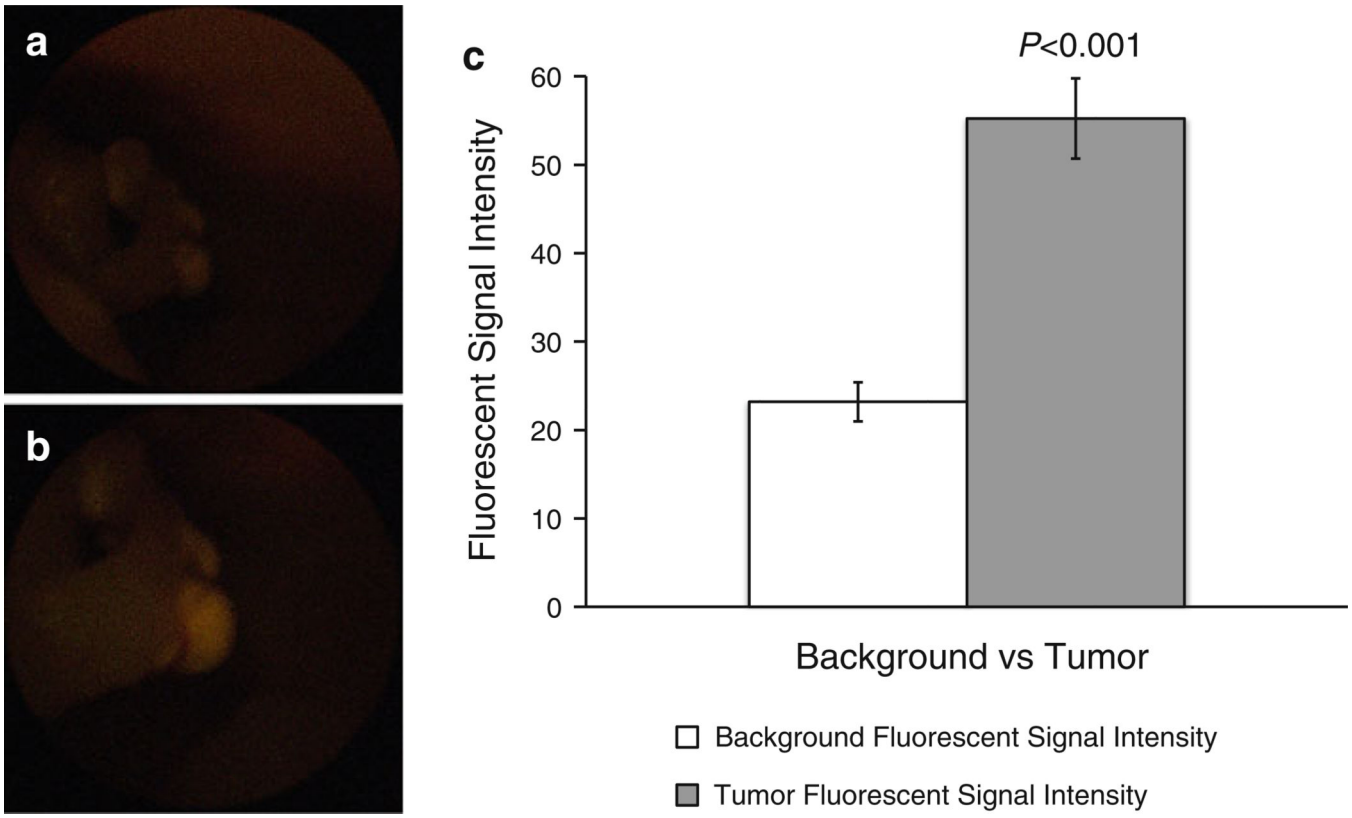

FIG. 2.

Fluorescence laparoscopy detects Alexa 488-labeled GISTs. Fluorophore-conjugated anti-KIT antibodies combined with fluorescence laparoscopy permitted enhanced detection and localization of cecal GISTs in the transgenic mouse model. Laparoscopic images of a cecal GIST from the same mouse labeled with anti-KIT antibodies demonstrate different fluorescence signal intensities of the (**a**) background and (**b**) 488-labeled GIST. c Enhanced contrast between tumor and normal bowel (e.g., background) is quantified. Signal intensity is calculated using ImageJ from laparoscopic images

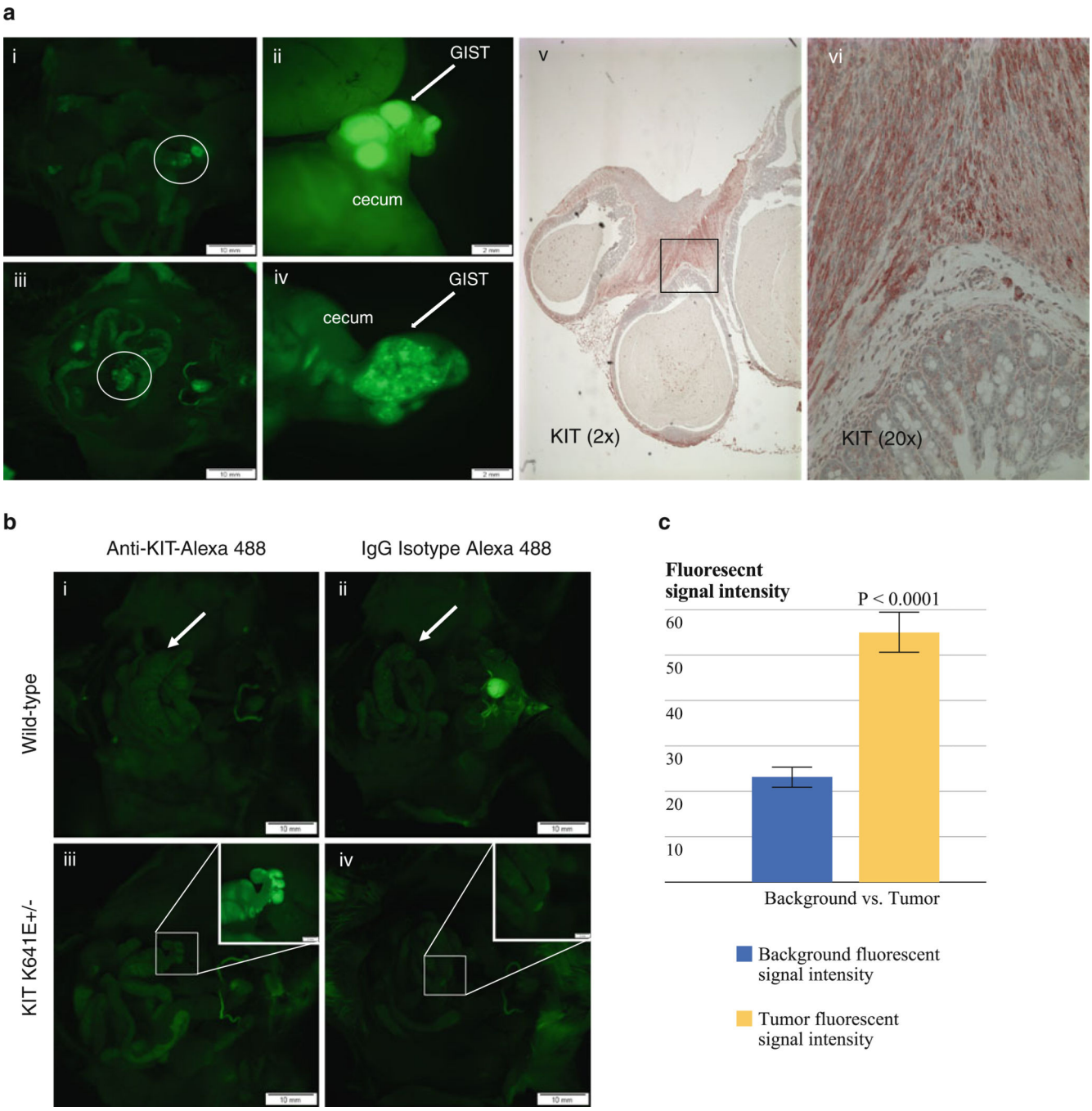

FIG. 3.

In vivo fluorescence labeling of GIST with anti-KIT Alexa 488 antibody vs. IgG isotype Alexa 488 antibody. **a** (*i*) and (*iii*) are wholebody images of 2 transgenic mice with fluorescently labeled cecal GISTs. The circles identify the location of tumors. (*ii*) and (*iv*) are magnified images of these circled cecal GISTs which better illustrate the specificity of the Alexa 488-conjugated antibody in labeling GISTs. (*v*) KIT staining (brown) of the cecal GIST, with corresponding magnified view (*vi*), from the $K641E^{+/-}$ mouse labeled with Alexa 488 [imaged in (*i*) and (*ii*)] confirms the presence of a GIST. (*i*/*iii*) Intravital images

of 2 transgenic mice with fluorescently labeled cecal GISTs (circles) were assessed using an OV-100 Imager. (*ii/iv*) Magnified images of cecal GISTs illustrate the specificity of Alexa 488-conjugated antibody in labeling GISTs. (*v/vi*) Photomicrographs (*v*, 2× and *vi*, 20×) of KIT immunostaining for the cecal tumors imaged in panels *i/ii*. **b** Intravital images taken of wild-type mice injected with (*i*) anti-KIT Alexa 488 antibody or (*ii*) IgG isotype control antibody. Given that wild-type mice do not develop cecal GISTs, these mice serve as a negative control in order to test the specificity of the antibody. Fluorescence signal is not seen at the cecum (white arrows). Transgenic mice were injected with either anti-KIT-Alexa 488 antibody or IgG isotype control-Alexa 488 antibody. Injection of the IgG antibody served as a negative control for the anti-KIT-Alexa 488 antibody. (*iv*) The cecal GIST is not fluorescently labeled in this mouse. (*iii*) In contrast, anti-KIT-Alexa 488 antibody labels the cecal GIST as evidenced by the presence of bright fluorescence signal

TABLE 1

Detection of GIST by bright light review

Animal	Antibody	No. of mice	No. of tumors detected	Tumor present on H&E
KIT K641E$^{+/-}$	KIT	4	4	4 (100 %)
KIT K641E$^{+/-}$	IgG[a]	3	3	3 (100 %)
Wild-type[b]	KIT	3	0	0 (0 %)
Wild-type[b]	IgG	3	0	0 (0 %)

GIST Gastrointestinal stromal tumor, *H&E* hematoxylin and eosin staining

[a] IgG isotype Alexa 488 labeling of GIST served as a negative control to anti-KIT-Alexa 488 antibody

[b] Wild-type mice served as a negative control to the KIT K641E$^{+/-}$ mice

TABLE 2

Detection of GISTs by fluorescence review

Animal	Antibody	No. of mice	No. of tumors detected with 488-labeling	Tumor present on H&E
KIT K641E$^{+/-}$	KIT	4	4	4 (100 %)
KIT K641E$^{+/-}$	IgG[a]	3	1 (FP)	3 (100 %)
Wild-type[b]	KIT	3	0	0 (0 %)
Wild-type[b]	IgG	3	1 (FP)	0 (0 %)

GIST Gastrointestinal stromal tumor, *H&E* hematoxylin and eosin staining, *FP* false-positive

[a] IgG isotype Alexa 488 labeling of GIST served as a negative control to anti-KIT-Alexa 488 antibody

[b] Wild-type mice served as a negative control to the K641E$^{+/-}$ mice